DMD Fast Forward. Published on February 28, 2017 as DOI: 10.1124/dmd.116.074500
This article has not been copyedited and formatted. The final version may differ from this version.

DMD # 74500

Effect of Disease-Related Changes in Plasma Albumin on the Pharmacokinetics of Naproxen in Male and Female Arthritic Rats

Xiaonan Li, Debra C DuBois, Richard R Almon, William J Jusko

Clinical Pharmacokinetics Laboratory, School of Basic Medicine and Clinical Pharmacy, China Pharmaceutical University, Nanjing, Jiangsu, 211198, China (XL); Department of Pharmaceutical Sciences, School of Pharmacy and Pharmaceutical Sciences, State University of New York at Buffalo, Buffalo, NY, 14214, USA (XL, DCD, RRA, WJJ); Department of Biological Sciences, State University of New York at Buffalo, Buffalo, NY, 14260, USA (DCD, RRA)

DMD Fast Forward. Published on February 28, 2017 as DOI: 10.1124/dmd.116.074500
This article has not been copyedited and formatted. The final version may differ from this version.

DMD # 74500

Running title: Naproxen pharmacokinetics in arthritic rats

Corresponding author:

William J Jusko, Ph.D.

Department of Pharmaceutical Sciences

School of Pharmacy and Pharmaceutical Sciences

State University of New York at Buffalo

Buffalo, NY, 14214

Telephone: 716-645-2855

Fax: 716-829-6569

E-mail: wjjusko@buffalo.edu

Number of text pages: 17

Number of tables: 4

Number of figures: 7

Number of references: 43

Number of words:

Abstract: 246

Introduction: 725

Discussion: 1462

ABBREVIATIONS: AUC, area under the plasma concentration time curve; CIA, collagen-induced arthritis; COX, cyclooxygenase; CYP, cytochrome P450; CV%, coefficient of variation; EDTA, ethylenediaminetetraacetic acid; ELISA, enzyme linked immunosorbent assay; GI, gastrointestinal; IP, intraperitoneally; IS, internal standard; ISF, interstitial fluid; LC-MS/MS, liquid chromatography-tandem mass spectrometry; NCA, non-compartmental analysis; NPX, naproxen; NSAIDs, nonsteroidal anti-inflammatory drugs; PBS, phosphate buffered saline; PD, pharmacodynamics; PK, pharmacokinetics; PG, prostaglandins; RA, rheumatoid arthritis; 2CM, two-compartment model.

ABSTRACT

Naproxen (NPX) is used in the treatment of rheumatoid arthritis (RA) for alleviation of pain and inflammation. In view of the extensive albumin binding of NPX, this study investigates whether chronic inflammation and sex will influence the physiological albumin concentrations, plasma protein binding, and pharmacokinetics (PK) of NPX. The PK of NPX was evaluated in a rat model of RA (collagen-induced arthritis (CIA) in Lewis rats) and in healthy controls. These PK studies included: 1) NPX in female and male CIA rats that received 10, 25 or 50 mg/kg NPX intraperitoneally (IP), and 2) NPX in healthy female and male rats after IP dosing of NPX at 50 mg/kg. Plasma albumin concentrations were quantified by ELISA and protein binding assessed using ultrafiltration. The NPX concentrations in plasma and filtrates were determined by LC-MS/MS. Plasma concentration-time data of NPX were first assessed by non-compartmental analysis (NCA). Nonlinear PK as indicated by dose-dependent NCA clearances and distribution volumes was observed. A two-compartment model (2CM) with a first-order absorption process incorporating nonlinear protein binding in plasma and tissues jointly described the PK data of all groups. Saturable albumin binding accounts for the nonlinearity of NPX PK in all rats as well as part of the PK differences in arthritic rats. The CIA rats exhibited reduced albumin concentrations, reduced overall protein binding, and reduced clearances of unbound NPX, consistent with expectations during inflammation. The net effect of chronic inflammation was an elevation of the C_{max} and AUC of unbound drug.

DMD Fast Forward. Published on February 28, 2017 as DOI: 10.1124/dmd.116.074500
This article has not been copyedited and formatted. The final version may differ from this version.

Introduction

Rheumatoid arthritis (RA) is a chronic systemic inflammatory autoimmune disease. It produces joint pain, stiffness, and swelling due to synovial inflammation and effusion. There is a sex preference with more women affected than men (van Vollenhoven, 2009). The pathogenesis of RA involves the biosynthesis and actions of many pro-inflammatory mediators including cytokines and prostaglandins (PG) (McInnes and Schett, 2011). In particular, PG play a key role in the generation of cardinal signs of acute inflammation such as pain, fever, redness and swelling by promoting blood flow into the inflamed tissues and increasing microvascular permeability (Funk, 2001; Ricciotti and FitzGerald, 2011), and also contribute to chronic inflammation through amplifying cytokine signaling as well as inducing and recruiting inflammatory cells at affected sites (Aoki and Narumiya, 2012).

Nonsteroidal anti-inflammatory drugs (NSAIDs) are extensively used to treat inflammatory diseases, including RA, because of their effective analgesic and anti-inflammatory properties (Crofford, 2013). The primary pharmacological mechanism of NSAIDs is blocking the biosynthesis of PG from arachidonic acid through inhibition of the enzymatic activity of cyclooxygenase (COX). There are two distinct isoforms. COX-1 is a constitutive enzyme that synthesizes PG to help maintain homeostatic functions including protection of gastric mucosa and platelet activation. In contrast, the expression of COX-2 is inducible under inflammatory conditions and serves as the main source of PG responsible for various inflammatory responses (Crofford et al., 2000; Smith et al., 2000; Ricciotti and FitzGerald, 2011). Despite the clinical effectiveness of NSAIDs, their side effects such as gastrointestinal (GI) bleeding and potential cardiovascular toxicity were also associated with the strong inhibition of either COX-1 or COX-2 (Lanas, 2009; Coxib et al., 2013).

Naproxen (NPX), a traditional NSAID, has been widely used in the management of RA (Davies and Anderson, 1997). It is a non-selective COX inhibitor that shows inhibitory effects for both isoforms with moderate potencies (Vane, 1971). Compared with selective COX inhibitors, NPX is better tolerated with respect to GI complications and cardiovascular risk (Lussier et al., 1978; Watson et al., 2002). Like most NSAIDs, NPX is highly bound to human plasma proteins especially albumin with very strong binding

(>99%) at therapeutic concentrations (Mortensen et al., 1979). Hypoalbuminemia frequently occurs in RA owing to increased catabolism (Wilkinson et al., 1965) and thereby the disposition of highly albumin bound drugs might be altered during RA. The clearance and distribution volume of NPX both increased in RA patients compared with normal subjects due to higher unbound NPX concentrations (van den Ouweland et al., 1987). Nonlinear pharmacokinetics (PK) caused by saturation of albumin binding at high total drug concentrations were reported (Stoeckel et al., 1981; Lin et al., 1985; Wong et al., 1999). Dose-dependent clearance of total drug and a plateau effect on the plasma concentration-time curve (AUC) were shown at higher NPX doses in man (Runkel et al., 1974). Sodium naproxen is a Biopharmaceutical Classification System I compound with high solubility and permeability and good absorption has been found in healthy and RA subjects (van den Ouweland et al, 1987; Vree et al. 1993).

The PK of NPX has been assessed in various species (Lauroba et al., 1986; Huntjens et al., 2006; Huntjens et al., 2010; Elsinghorst et al., 2011). However, the underlying mechanisms causing the nonlinear PK have either been neglected or not been fully explored. The NPX PK profiles in earlier studies were described using simple linear clearance models without consideration of the nonlinearity. In addition, the influences of chronic inflammation (RA) and sex on the protein binding and disposition of NPX have not yet been well investigated. Our studies are consonant with recent emphasis (Danska, 2014) that translational studies of sex differences should be expanded.

Collagen-induced arthritis (CIA) in Lewis rats is an animal disease model that closely resembles many features of human RA (Stuart et al., 1982; Holmdahl et al., 2001). This model has been successfully applied to assess the PK/Pharmacodynamic (PD) properties of various drugs including dexamethasone, anakinra, and abatacept (Earp et al., 2008b; Liu et al., 2011; Lon et al., 2013).

In the current study, the PK of NPX was examined in female and male normal and CIA rats after various intraperitoneal (IP) doses of NPX. A global PK model incorporating sex and disease effects on nonlinear protein binding was successfully applied. This study was designed to support a subsequent preclinical PD study of NPX in CIA rats (Li et al, 2017).

Materials and Methods

Reagents and chemicals. Naproxen (purity >98.5%), sodium naproxen, LC-MS grade acetonitrile, and HPLC-grade formic acid were all obtained from Sigma-Aldrich Inc. (St Louis, MO). (S)-Naproxen-d3 (internal standard (IS), purity >98%) was purchased from Toronto Research Chemicals Inc. (Toronto, Canada). Milli-Q® water was used (Millipore Corporation, Bedford, MA).

Animals. Male and female Lewis rats (5-8 weeks old) were purchased from Harlan (Indianapolis, IN), weighing approximately 110 to 160 g for females and 170 to 220 g for males, age-matched for each sex group at the time of PK studies. All rats were housed individually in the University Laboratory Animal Facility under controlled temperature (22°C) and humidity, 12-h light/12-h dark cycles, and free access to water and food. Rats were acclimated for 1 week before studies. These studies were performed in accordance with the Guide for the Care and Use of Laboratory Animals (Institute of Laboratory Animal Resources, 2011) and were approved by the University at Buffalo Institutional Animal Care and Use Committee.

Induction of CIA in Lewis Rats. The induction of CIA in Lewis rats was conducted following protocols and reagents supplied by Chondrex (Redmond, WA). The detailed procedures were as previously described (Earp et al., 2008a). Paw edema and body weights were monitored from the first day of induction through day 15 for females and day 20 for males. Hind paw swelling was used as the indicator for edema and measured by digital calipers (VWR Scientific, Rochester, NY). The peak disease status was observed on day 16 for females and day 21 for males. Approximately 60% of the males and 80% of the females successfully developed arthritis in one or both hind paws.

Pharmacokinetics of NPX. The NPX doses were prepared freshly as a sodium NPX solution in phosphate buffered saline (PBS) (pH=8), and filtered through 0.22 micron filters before use. The drug was administered intraperitoneally (IP) in a volume of 1 mL/kg.

The female and male CIA rats were randomly divided into 3 subgroups per sex group and received an IP bolus injection with 11, 27.5 or 55 mg/kg of sodium NPX PBS solution (equivalent to 10, 25 or 50 mg/kg of NPX) on day 16 (females) and day 21 (males) post disease induction. Healthy male and female

rats were dosed IP with 55 mg/kg of sodium NPX in PBS (50 mg/kg of NPX). Serial blood samples were collected from the saphenous vein using ethylenediaminetetraacetic acid (EDTA) as the anticoagulant at 15, 30 and 45 min and 1, 2, 4, 6, 9, 12, 24 h post-dose. There were 3 CIA rats and 4 healthy rats sampled at each time point. Blood samples were immediately centrifuged at 2000 × g for 15 min at 4°C and the obtained plasma samples were stored at –80°C before analysis.

Blood Collection for Albumin and Protein Binding. Eight CIA females and 8 healthy females were sacrificed on day 16 after arthritis induction by aortal exsanguinations under isoflurane anesthesia. Four CIA males and 4 healthy males were sacrificed on day 21 after induction. Blood samples were collected into syringes pre-coated with EDTA and centrifuged immediately at 2000 × g for 15 min at 4°C. Plasma samples were collected and 25 µL of the plasma from each rat was separated and stored for albumin determination. The remaining fractions were pooled for each animal group and used in subsequent protein binding studies.

Plasma Albumin Determination. The plasma concentrations of albumin in CIA and healthy rats (both sex groups) were quantified using an anti-rat albumin enzyme linked immunosorbent assay (ELISA) kit (Bethyl Laboratories, Montgomery, TX). Rat plasma samples were diluted (1:1,000,000) by conjugate diluent prior to assay. All other procedures followed the manufacturer's protocol. Four rats from each animal group were used and all samples were run in triplicate. The range of the standard curve was 1.95-125 ng/mL and a four-parameter logistic model was applied to fit the standard curve.

Plasma Protein Binding of NPX. Plasma protein binding of NPX was measured by ultrafiltration using Centrifree micropartition devices (Millipore Corporation, Bedford MA) with a 30 kDa molecular weight cut-off filter. Briefly, 16 µL of NPX PBS solutions (0.2, 0.5, 1, 2, 5, 10, 20 and 50 mg/mL) were added at 1% of total volume to pooled blank plasma samples from each group to yield 8 plasma samples containing NPX per group (2, 5, 10, 20, 50, 100, 200 and 500 µg/mL). After incubation at 37°C for 30 min, aliquots (460 µL) of plasma of each concentration were transferred into 3 pre-rinsed ultrafiltration devices and centrifuged at 2000 ×*g* for 20 min. The filtrates and remaining plasma samples were stored at -80°C

until analysis of both free and total NPX concentrations. Preliminary studies showed that there was negligible nonspecific binding of NPX to the ultrafiltration device.

Drug Analysis. The NPX concentrations in all samples were determined by liquid chromatography-tandem mass spectrometry (LC-MS/MS). Briefly, plasma samples (15 μL) from the PK and protein binding studies were spiked with 10 μL of IS working solutions (2.5 μg/mL) followed by precipitation with 400 μL of acetonitrile containing 0.1% of formic acid. The mixtures were vortexed for 1 min and sonicated for 20 s, then vortexed for another 10 s after sonication and centrifuged at 13000 ×*g* for 10 min. Then 300 μL of the supernatant were transferred to a 2-mL tube containing 1.2 mL of water and vortexed for 10 s. Finally, 10 μL of the mixture were injected onto the LC-MS/MS for analysis.

The NPX concentrations in the filtrates (free drug concentrations) from the protein binding studies were pretreated using the same method as plasma samples with slight modifications. Briefly, 75 μL of each filtrate sample was spiked with 10 μL of IS working solutions (2.5 μg/mL) followed by precipitation with 300 μL of acetonitrile containing 0.1% of formic acid. The remaining sample preparation procedures were as described above for the plasma samples.

The LC-MS/MS system consisted of a Shimadzu HPLC module including a binary pump, a degasser, an auto-sampler and a column oven (Kyoto, Japan), and an Applied Biosystems PE/Sciex API3000 mass spectrometer equipped with a turbo ion spray interface (Foster City, CA). Sample separations were achieved on a Targa C18 Column (particle size 5 μm, 100 × 2.1 mm; Higgins Analytical Inc., Mountain View, CA). The mobile phase consisted of eluent A (water/acetonitrile (95:5 v/v) containing 0.1% acetic acid) and eluent B (acetonitrile/water (95:5 v/v) containing 0.1% acetic acid) and was pumped at a flow rate of 0.23 mL/min with a gradient elution. The gradient profile was as follows: 0-4 min, 50% B; a linear increase to 95% B from 4 to 6.5 min; a linear decrease to 50% B over 0.1 min; 50% B for 4.4 min; and stop at 11.00 min. The auto-sampler was maintained at 4°C during the run. The mass spectrometer was operated in the negative ionization mode for the detection of ion transitions at m/z 229.2/169.9 for NPX and 232.0/169.9 for IS. The system was controlled by Analyst software version 1.4 (Applied Biosystems SciEx) for data acquisition and analysis.

DMD Fast Forward. Published on February 28, 2017 as DOI: 10.1124/dmd.116.074500
This article has not been copyedited and formatted. The final version may differ from this version.

Linearity was found over the concentration ranges of 0.125 to 40 μg/mL for plasma and 0.01 to 30 μg/mL for filtrate samples. The coefficient of variation (CV%) of intra- and inter-day accuracies and precisions were all with CV% <10%. The recovery of the sample preparation method approached 100%. Naproxen in rat plasma was previously found to be stable under various conditions (Shi et al., 2015).

Protein Binding and Pharmacokinetic Data Analysis. The binding capacity and association constants were estimated by fitting the bound versus free drug concentrations using an equation describing two classes of binding sites (Wong et al., 1999):

$$C_{bp} = \frac{n_1 Pt \cdot K_{a1} \cdot C_{up}}{1 + K_{a1} \cdot C_{up}} + \frac{n_2 Pt \cdot K_{a2} \cdot C_{up}}{1 + K_{a2} \cdot C_{up}} \quad (1)$$

where C_{bp} and C_{up} are the bound and free plasma NPX concentrations; Ka_1 and Ka_2 are the association constants for the first and second class of binding sites; n_1 and n_2 are the numbers of first and second class binding sites; and Pt is the albumin concentration in plasma.

The relationship between bound and total drug concentrations is:

$$C_{bp} = C_p - C_{up} \quad (2)$$

where C_p is the total plasma concentration of NPX.

Based on the assessment of the plasma protein binding data, $K_{a2} \cdot C_{up} \ll 1$, and substitution for bound concentrations using equation (2) yields:

$$(n_2 Pt \cdot K_{a2} \cdot K_{a1} + K_{a1}) \cdot C_{up}^2 + \left(n_1 Pt \cdot K_{a1} + n_2 Pt \cdot K_{a2} - C_p \cdot K_{a1} + 1\right) \cdot C_{up} - C_p = 0 \quad (3)$$

where there is one positive root for free drug concentration:

$$C_{up} = \left(-\left(n_1 Pt \cdot K_{a1} + n_2 Pt \cdot K_{a2} - C_p \cdot K_{a1} + 1\right) + \sqrt{4 \cdot (n_2 Pt \cdot K_{a2} \cdot K_{a1} + K_{a1}) \cdot C_p + \left(n_1 Pt \cdot K_{a1} + n_2 Pt \cdot K_{a2} - C_p \cdot K_{a1} + 1\right)^2}\right) / 2 \cdot (n_2 Pt \cdot K_{a2} \cdot K_{a1} + K_{a1}) \quad (4)$$

The protein binding of NPX in tissues is considered to occur primarily to albumin in the interstitial fluid (ISF) (Aukland and Nicolaysen, 1981; Rodgers and Rowland, 2006). Assuming that the binding affinities and numbers of binding sites on each protein molecule in ISF is the same as in plasma, then the

DMD Fast Forward. Published on February 28, 2017 as DOI: 10.1124/dmd.116.074500
This article has not been copyedited and formatted. The final version may differ from this version.

relationship between total (C_t) and unbound tissue concentrations (C_{ut}) of NPX could also be described by Eq. (4) with a difference in ISF and plasma protein concentrations where Pt is multiplied by *E/P*, the ratio of protein concentrations in ISF and plasma.

According to the "Free Hormone Hypothesis" (Mendel, 1989), disposition processes often operate only on free drug. Therefore, NPX plasma concentration-time profiles were characterized by compartment models based on free drug concentrations with binding calculated from total concentrations. Several models including one- and two-compartment PK models (with or without an absorption process) with binding were tested, and the final PK model selected (Figure 1) was a two-compartment model with first-order absorption process incorporating nonlinear protein binding. The final PK model equations and initial conditions are:

$$\frac{dA_a}{dt} = -k_a \cdot A_a\,, \qquad A_a(0) = \text{Dose} \cdot F \tag{5}$$

$$V_p \cdot \frac{dC_p}{dt} = k_a \cdot A_a + CL_d \cdot \left(C_{ut} - C_{up}\right) - CL \cdot C_{up}, \qquad C_p(0) = 0 \tag{6}$$

$$V_t \cdot \frac{dC_t}{dt} = CL_d \cdot (C_{up} - C_{ut}), \qquad C_t(0) = 0 \tag{7}$$

where A_a indicates the amount of NPX at the absorption site, k_a is the first-order absorption rate constant, *CL* and CL_d are the plasma and distribution clearances of unbound NPX, V_p and V_t are the volumes of distribution of total NPX in central and peripheral compartments, and *F* is the bioavailability of the IP dose calculated to be about 0.9 from literature-reported IV data in rats (Lauroba et al., 1986). The drug was given IP to minimize stress in the animals and based on observations that NPX absorption is rapid, reproducible, and essentially complete by this route (Huntjens et al, 2006).

Initial non-compartmental analysis (NCA) of the PK data was performed using the Phoenix WinNonlin 6.4 software (Certara Corporation). All model fittings were performed using the maximum likelihood algorithm in ADAPT 5 (BMSR, CA) (D'Argenio et al., 2009). The model code is provided in the Supplementary Materials. All protein binding and PK data were naive-pooled before analysis. The protein binding profiles were first fitted and the estimated binding parameters were fixed in the PK model. The variance model used was:

$$V_i = (\sigma_1 + \sigma_2 \cdot Y_i)^2 \tag{8}$$

where V_i represents the variance of the ith data point and Y_i is the ith model predicted plasma concentration. σ_1 and σ_2 are variance model parameters and were estimated together with other system parameters during model fitting. Model selection was based on the goodness-of-fit criteria which included the Akaike Information Criterion (AIC), visual inspection of the fitted profiles, and Coefficients of Variation (CV%) of the parameter estimates.

Statistical analysis. All data were analyzed statistically by one-way analysis of variance and Tukey's multiple comparison test using SPSS software version 22 (IBM SPSS Statistics, Chicago, IL, USA), and $p < 0.05$ was considered to be statistically significant.

Results

Quantification of Plasma Albumin. An anti-rat albumin ELISA was applied to determine whether sex and the presence of arthritis influence the plasma concentrations of albumin. As shown in both Figure 2 and Table 1, the plasma albumin concentrations in CIA rats were significantly lower than those in healthy animals, consistent with the situation in humans that hypoalbuminemia is a feature of RA (Wilkinson et al., 1965). It is interesting to note that albumin concentrations also differed significantly with sex in rats with lower values observed in males.

Protein Binding of NPX. Protein binding studies of NPX were carried out using plasma from the four animal groups. Plasma protein binding of NPX in rats showed concentration-dependence, with higher unbound fractions at higher total plasma concentrations (Figure 3). Higher percent binding of NPX to rat plasma proteins (> 93%) was observed at normal therapeutic concentrations in all groups with very small variation (CV% < 2.36%). However, a significant decrease in binding was found at total concentrations greater than 50 µg/mL in CIA rats and above 100 µg/mL in healthy rats (Supplemental Table S1). Rosenthal plots (Figure 3) presenting the bound/unbound drug concentration ratios versus bound concentrations showed biphasic profiles, indicating that there are two classes of binding sites on the protein. The bound versus free concentration profiles were fitted to the binding equation with two classes of binding sites (Eq. 1) (Supplemental model code for protein binding). Preliminary fittings allowing n_1 and n_2 to vary yielded the nearest integers of 1 and 4, which were then fixed for subsequent assessment. As shown in Figure 4, there was a very good agreement between the observed and fitted data except that the bound concentrations in CIA males were slightly under predicted at the highest free concentrations. The association constants listed in Table 2 indicate that NPX is bound to rat plasma albumin with high affinity, and the first class (n_1) of binding sites differed from the second (n_2) as Ka_2 was only about 2% of Ka_1. In addition, the binding capacities (nPt) varied with lower binding capacities in the CIA rats and male rats (Table 1).

Pharmacokinetics of NPX. The PK of NPX was investigated in CIA rats and compared with that in healthy animals. Following IP doses of NPX (10, 25 and 50 mg/kg) to CIA rats and 50 mg/kg to healthy rats, the NPX PK profiles of all groups shown in Figures 5 and 6 were bi-exponential with parallel

elimination phases between the dose groups. A sharper initial decline was observed in higher dose groups, indicating that distribution rates increased with dose/concentration. The primary PK parameters for total drug were initially calculated by NCA for comparison with published PK results. In CIA rats, plasma NPX concentrations increased less than dose-proportionally in both sex groups, as indicated by the dose-normalized AUC, which decreased by nearly 2-fold over the 5-fold range of doses. In addition, the apparent volume of distribution (*V/F*) and apparent clearance (*CL/F*) significantly increased in the highest dose groups (50 mg/kg) compared to those in the 10 mg/kg dose groups (Table 3). Together, these results indicated the occurrence of dose-dependent PK of NPX in CIA rats. The NCA results for arthritic and healthy rats are listed in Table 4. The AUC of total NPX in arthritic rats was significantly lower than that in healthy animals. Both *V/F* and *CL/F* values in CIA rats were about 30-50% higher than the corresponding values in healthy rats. Despite these differences, NCA did not indicate any significant differences in the PK parameters between female and male rats. In addition, the terminal half-life ($t_{1/2}$) was similar in all dose groups in CIA rats and between arthritic and healthy rats at the same dose level (Tables 2 and 3). The apparent clearance values for NPX are considerably smaller than hepatic plasma flow (circa 1200 ml/h/kg) (Davies and Morris, 1993) indicating that this is a low clearance compound and should have little first-pass loss after IP administration.

A two-compartment model with a first-order absorption process and nonlinear albumin binding (Figure 1) was used to describe the PK of NPX (Supplemental model code for PK estimation). Free NPX concentrations calculated from the total using the protein binding parameters in Table 1 were used in modeling (Eq. 5-7) (Supplemental model code for PK simulation). The model fittings applied jointly for all animals and PK groups along with the corresponding model-predicted unbound plasma concentrations of NPX are shown in Figures 5 and 6. The final model parameter estimates are presented in Table 4. This model described the PK profiles reasonably well, except for missing the last time point, with low CV% values for all parameter estimates. Absorption of NPX from the IP injection site was rapid with a k_a value about 0.8 h^{-1}, which is in line with reported data (Huntjens et al, 2006; Huntjens et al, 2010). The CIA rats showed lower unbound plasma clearances ($CL_{\text{Arthritic}}$) and larger peripheral distribution volumes of total

DMD Fast Forward. Published on February 28, 2017 as DOI: 10.1124/dmd.116.074500
This article has not been copyedited and formatted. The final version may differ from this version.

drug ($V_{t\ Arthritic}$) compared with healthy rats, consistent with the findings in humans (van den Ouweland et al., 1987). The estimated V_t values approach the ISF volume in rats (174 mL/kg) (Shah and Betts, 2012), further indicating that NPX distributes principally to tissue interstitial space. Lower unbound distribution clearances in CIA rats ($CL_{d\ Arthritic}$) observed in our study also agrees with previous findings indicating that the rheumatoid synovium is less permeable to small molecules and inflammation might decrease the distribution of unbound NSAIDs into and out of tissues (Simkin, 1979; Wallis et al., 1985; Day et al., 1999). It is apparent that NPX is a low extraction drug and its unbound plasma clearance is mainly determined by the intrinsic clearance based on the well-stirred model of hepatic clearance. The unbound plasma NPX concentration-time profiles for all 50 mg/kg dose groups are shown in Figure 7. In both sex groups, arthritic rats showed higher peak unbound concentrations (13.52 *vs.* 8.14 μg/mL for females and 13.51 *vs.* 8.43 μg/mL for males) and increased unbound AUC (32.76 *vs.* 23.94 μg·h/mL for females and 32.82 *vs.* 23.95 μg·h/mL for males) compared with healthy rats.

Discussion

Protein binding has been known play a substantial role in the PK and PD of NSAIDs (Lin et al., 1987). NPX is an acidic NSAID that is extensively bound to albumin (>99%) within the normal therapeutic range in plasma (20~200 μg/mL) (Mortensen et al., 1979). Different plasma albumin concentrations and binding kinetics of NPX with disease and sex, along with altered intrinsic clearances affected the disposition of NPX.

We found lower albumin concentrations along with nonlinear NPX PK in arthritic rats producing a disproportionate increase of AUC with dose. This phenomenon occurs in humans, where the AUC of NPX tended to plateau at higher doses (500 to 900 mg, which are about 45 to 80 mg/kg in rats) (Runkel et al., 1974). The absorption of NPX is rapid and complete (Runkel et al., 1974; Segre, 1975) and NPX absorption in RA patients is similar to healthy subjects (van den Ouweland et al., 1987; Vree et al., 1993). Therefore**,** the explanation for the plateau effect in AUC was a greater clearance at high doses due to elevated free drug concentrations resulting from saturation of albumin binding (Mortensen et al., 1979; Calvo and Dominguezgil, 1983). Under inflammatory conditions, albumin is also subject to increased catabolism (Wilkinson et al., 1965). Altered albumin binding in RA results in more free drug available for elimination, leading to lower AUC and higher *CL* in both RA patients and CIA rats given the same dose levels. Thus, different PK behaviors were expected between healthy and arthritic rats, in accordance with findings in humans (van den Ouweland et al., 1987). Although $t_{1/2}$ did not change with dose or disease, this parameter was determined by concentrations falling within the linear protein binding range.

As seen from the ELISA results, plasma albumin concentrations differed significantly with disease and sex with lower values in CIA rats and in male rats. A negative correlation was found between the NCA values of *CL/F* and plasma albumin concentrations in all groups (r = 0.94), and the values of *V/F* in both sex groups were also inversely related to plasma albumin concentrations. These results confirmed that chronic inflammation reduced plasma albumin and partly influenced the PK of NPX. However, different albumin concentrations between female and male rats did not produce differences in PK, suggesting that other factors (e.g. drug metabolism) are involved.

DMD Fast Forward. Published on February 28, 2017 as DOI: 10.1124/dmd.116.074500
This article has not been copyedited and formatted. The final version may differ from this version.

This study was enacted to further explore and comprehensively integrate and model the role of different plasma albumin concentrations on the binding of NPX, to examine whether nonlinear protein binding accounts for the nonlinearities in NPX PK, and assess disease and sex effects. The bound fractions of NPX in our study are slightly higher than other data in rats (Huntjens et al., 2006). In our study, protein binding of NPX was constant at low drug concentrations and became saturated at higher concentrations. Such saturation of binding was observed at lower NPX concentrations in CIA rats, which can be explained by their lower albumin concentrations. In CIA rats, even with very small decreases in percent bound, the unbound fractions of NPX can vary up to about 6-fold over the therapeutic concentration range, which is comparable to the situation in humans (Borga and Borga, 1997). Our companion study assesses whether the pharmacological effects of NPX can be directly related to the unbound drug concentrations in CIA rats (Li et al, 2017).

Initial modeling tests showed that the estimated number of binding sites n_1 and n_2 were close to 1 and 4, in all groups except CIA males where the estimated n_2 value was 6.6. Nonetheless, uniform values of n (n_1 =1 and n_2=4) were chosen for all groups in the final model and only the association constants (Ka_1 and Ka_2) were estimated. The binding affinity of NPX to one class of binding site on albumin was much higher than the other. Attempted modeling of all protein binding data using single values for Ka_1 and Ka_2 produced less satisfactory overall fittings. The lower binding capacity observed in CIA rats and in male rats was primarily due to their lower albumin concentrations.

From the perspective of mechanism, albumin and drug concentration-dependent protein binding was incorporated into a classic type of 2CM to account for the nonlinearity of NPX PK. This modeling approach is based on the literature (Fleishaker and McNamara, 1985) in that free drug was used to govern the distribution process of total drug. However, their model only applies when protein binding and clearance are linear. Our model is more comprehensive in accounting for nonlinear binding in plasma and tissues, operating both distribution and elimination processes using unbound drug, and featuring a global analysis of all experimental data jointly. These advantages offset our ability to capture all data perfectly, especially the last time point, which differs from the fitting trend for unknown reasons.

Protein concentrations in tissue interstitial space are known to increase due to the increase of microvascular permeability with inflammation (Aukland and Johnsen, 1974; Simkin, 1979; Bell et al., 1983); therefore, different *E/P* values were assigned to CIA and healthy rats. The average *E/P* based on the literature is about 0.5 for healthy rats (Rodgers et al., 2005; Rodgers and Rowland, 2006). Assuming that increased albumin concentrations in CIA ISF is mainly attributed to the transfer of albumin from plasma to ISF, the *E/P* value used for CIA rats was about 0.9 based on the reduced fraction of plasma albumin concentrations. This is in accordance with findings in humans that *E/P* is about 0.32 in healthy subjects and increases to about 0.73 in RA patients (Fleishaker and McNamara, 1985; Day et al., 1995). Since no significant alteration of the absorption of NPX occurs with RA (van den Ouweland et al., 1987; Vree et al., 1993), the absorption rate constant (k_a) was shared for all groups. The central distribution volume of total drug (V_p) was difficult to estimate perhaps owing to the IP doses and thus it was fixed to rat plasma volume to improve model stability. In the final model, different values of unbound plasma clearances (CL), unbound distribution clearances (CL_d) and peripheral distribution volumes of total drug (V_t) were assigned for CIA and healthy rats. The presence of pro-inflammatory mediators during inflammation is commonly associated with reduced CYP expression and activity, leading to impaired drug metabolism (Slaviero et al., 2003; Renton, 2005). Therefore, the lower value of $CL_{Arthritic}$ was expected as NPX undergoes significant hepatic metabolism that is primarily dependent on cytochromes CYP2C9 and CYP1A2 (Miners et al., 1996). The effects of chronic inflammation on the tissue disposition of NPX still remain unclear. However, it might be anticipated that the diffusion of unbound NPX into and out of tissues should decrease due to decreased perfusion with inflammation (Wallis et al., 1985). The lower unbound distribution clearance observed in CIA rats is consistent with this. The larger peripheral distribution volume of total NPX in CIA rats corresponded well with the NCA results. As the ISF protein concentrations increase with inflammation, the bound fraction of NPX will increase in ISF and thereby enhance the penetration of total drug into tissue as previously reported (Fleishaker and McNamara, 1985). The estimated V_t values of all groups were smaller than ISF volume, which might be due to collagen occupying part of the ISF space. The PK parameters based on free drug were independent of dose confirming that saturation of protein binding was the major

determinant of the dose-dependent PK in CIA rats. Despite the consistency of findings regarding the influences of RA on the disposition of total and unbound NPX, our results showed no significant sex effects. It was reported that females exhibited higher free NPX concentrations than male patients with osteoarthritis (Hundal et al., 1991).

The CIA rat model exhibits many similar histopathological features as human RA such as synovial proliferation, pannus formation, and cartilage destruction (Stuart et al., 1982). Therefore, the results of this study appear to mimic and explain the nonlinear PK of NPX in humans, as well as the effects of chronic inflammation and sex on the protein binding and disposition of NPX in RA patients.

In conclusion, plasma albumin concentrations in rats differed significantly with sex and arthritis, which leads to markedly different PK behaviors of NPX. Reduced albumin in plasma and altered protein binding of NPX was shown to be the primary cause for the dose-dependent PK of NPX in normal and arthritic rats, with the latter also exhibiting impaired clearance of free drug. The PK profiles of NPX in all groups were well-described by the global PK model incorporating these diverse factors. This is the most complete exploration of the nonlinear PK of NPX with comparisons based on sex and presence of disease. This study serves as the prelude for our subsequent pharmacodynamics study of NPX in CIA rats (Li et al, 2017).

Authorship contributions

Participated in research design: Li, DuBois, Almon, Jusko

Conducted experiments: Li, DuBois

Performed data analysis: Li, Jusko

Wrote or contributed to the writing of the manuscript: Li, DuBois, Almon, Jusko

References

Aoki T and Narumiya S (2012) Prostaglandins and chronic inflammation. *Trends Pharmacol Sci* **33:**304-311.

Aukland K and Johnsen HM (1974) Protein concentration and colloid osmotic pressure of rat skeletal muscle interstitial fluid. *Acta Physiol Scand* **91:**354-364.

Aukland K and Nicolaysen G (1981) Interstitial fluid volume: local regulatory mechanisms. *Physiol Rev* **61:**556-643.

Bell DR, Mullins RJ, and Powers MR (1983) Extravascular distribution of albumin and IgG during high-permeability edema in skin. *Am J Physiol* **244:**H599-606.

Borga O and Borga B (1997) Serum protein binding of nonsteroidal antiinflammatory drugs: a comparative study. *J Pharmacokinet Biopharm* **25:**63-77.

Calvo MV and Dominguezgil A (1983) Binding of Naproxen to Human-Albumin - Interaction with Palmitic Acid. *Int J Pharm* **16:**215-223.

Coxib, traditional NTC, Bhala N, Emberson J, Merhi A, Abramson S, Arber N, Baron JA, Bombardier C, Cannon C, Farkouh ME, FitzGerald GA, Goss P, Halls H, Hawk E, Hawkey C, Hennekens C, Hochberg M, Holland LE, Kearney PM, Laine L, Lanas A, Lance P, Laupacis A, Oates J, Patrono C, Schnitzer TJ, Solomon S, Tugwell P, Wilson K, Wittes J, and Baigent C (2013) Vascular and upper gastrointestinal effects of non-steroidal anti-inflammatory drugs: meta-analyses of individual participant data from randomised trials. *Lancet* **382:**769-779.

Crofford LJ (2013) Use of NSAIDs in treating patients with arthritis. *Arthritis Res Ther* **15 Suppl 3:**S2.

Crofford LJ, Lipsky PE, Brooks P, Abramson SB, Simon LS, and van de Putte LB (2000) Basic biology and clinical application of specific cyclooxygenase-2 inhibitors. *Arthritis Rheum* **43:**4-13.

Danska JS (2014) Sex matters for mechanism. *Sci Transl Med* **6:**258fs240.

Davies B and Morris T (1993) Physiological parameters in laboratory animals and humans. *Pharm Res* **10:**1093-1095.

Davies NM and Anderson KE (1997) Clinical pharmacokinetics of naproxen. *Clin Pharmacokinet* **32:**268-293.

Day RO, Francis H, Vial J, Geisslinger G, and Williams KM (1995) Naproxen concentrations in plasma and synovial fluid and effects on prostanoid concentrations. *J Rheumatol* **22:**2295-2303.

Day RO, McLachlan AJ, Graham GG, and Williams KM (1999) Pharmacokinetics of nonsteroidal anti-inflammatory drugs in synovial fluid. *Clin Pharmacokinet* **36:**191-210.

Earp JC, Dubois DC, Molano DS, Pyszczynski NA, Keller CE, Almon RR, and Jusko WJ (2008a) Modeling corticosteroid effects in a rat model of rheumatoid arthritis I: mechanistic disease progression model for the time course of collagen-induced arthritis in Lewis rats. *J Pharmacol Exp Ther* **326:**532-545.

Earp JC, Pyszczynski NA, Molano DS, and Jusko WJ (2008b) Pharmacokinetics of dexamethasone in a rat model of rheumatoid arthritis. *Biopharm Drug Dispos* **29:**366-372.

Elsinghorst PW, Kinzig M, Rodamer M, Holzgrabe U, and Sorgel F (2011) An LC-MS/MS procedure for the quantification of naproxen in human plasma: development, validation, comparison with other methods, and application to a pharmacokinetic study. *J Chromatogr B Analyt Technol Biomed Life Sci* **879:**1686-1696.

Fleishaker JC and McNamara PJ (1985) Performance of a diffusional clearance model for beta-lactam antimicrobial agents as influenced by extravascular protein binding and interstitial fluid kinetics. *Antimicrob Agents Chemother* **28:**369-374.

Funk CD (2001) Prostaglandins and leukotrienes: advances in eicosanoid biology. *Science* **294:**1871-1875.

Holmdahl R, Lorentzen JC, Lu S, Olofsson P, Wester L, Holmberg J, and Pettersson U (2001) Arthritis induced in rats with nonimmunogenic adjuvants as models for rheumatoid arthritis. *Immunol Rev* **184:**184-202.

Hundal O, Rugstad HE, and Husby G (1991) Naproxen free plasma concentrations and unbound fractions in patients with osteoarthritis: relation to age, sex, efficacy, and adverse events. *Ther Drug Monit* **13:**478-484.

Huntjens DR, Spalding DJ, Danhof M, and Della Pasqua OE (2006) Correlation between in vitro and in vivo concentration-effect relationships of naproxen in rats and healthy volunteers. *Br J Pharmacol* **148:**396-404.

Huntjens DR, Spalding DJ, Danhof M, and Della Pasqua OE (2010) Impact of chronic inflammation on the pharmacokinetic-pharmacodynamic relationship of naproxen. *Eur J Pain* **14:**227 e221-210.

Lanas A (2009) Nonsteroidal antiinflammatory drugs and cyclooxygenase inhibition in the gastrointestinal tract: a trip from peptic ulcer to colon cancer. *Am J Med Sci* **338:**96-106.

Lauroba J, Domenech J, Moreno J, and Pla-Delfina JM (1986) Relationships between biophasic disposition and pharmacokinetic behavior in nonsteroid antiinflammatory drugs. *Arzneimittelforschung* **36:**710-714.

Li N, DuBois DC, Almon RR, Jusko WJ (2017) Modeling sex differences in the pharmacokinetics, pharmacodynamics, and disease progression of naproxen in rats with collagen-induced arthritis, Submitted for publication.

Lin JH, Cocchetto DM, and Duggan DE (1987) Protein binding as a primary determinant of the clinical pharmacokinetic properties of non-steroidal anti-inflammatory drugs. *Clin Pharmacokinet* **12:**402-432.

Lin JH, Hooke KF, Yeh KC, and Duggan DE (1985) Dose-dependent pharmacokinetics of diflunisal in rats: dual effects of protein binding and metabolism. *J Pharmacol Exp Ther* **235:**402-406.

Liu D, Lon HK, Dubois DC, Almon RR, and Jusko WJ (2011) Population pharmacokinetic-pharmacodynamic-disease progression model for effects of anakinra in Lewis rats with collagen-induced arthritis. *J Pharmacokinet Pharmacodyn* **38:**769-786.

Lon HK, Liu D, DuBois DC, Almon RR, and Jusko WJ (2013) Modeling pharmacokinetics/pharmacodynamics of abatacept and disease progression in collagen-induced arthritic rats: a population approach. *J Pharmacokinet Pharmacodyn* **40:**701-712.

Lussier A, Arsenault A, and Varady J (1978) Gastrointestinal microbleeding after aspirin and naproxen. *Clin Pharmacol Ther* **23:**402-407.

McInnes IB and Schett G (2011) The pathogenesis of rheumatoid arthritis. *N Engl J Med* **365:**2205-2219.

Mendel CM (1989) The free hormone hypothesis: a physiologically based mathematical model. *Endocr Rev* **10:**232-274.

Miners JO, Coulter S, Tukey RH, Veronese ME, and Birkett DJ (1996) Cytochromes P450, 1A2, and 2C9 are responsible for the human hepatic O-demethylation of R- and S-naproxen. *Biochem Pharmacol* **51:**1003-1008.

Mortensen A, Jensen EB, Petersen PB, Husted S, and Andreasen F (1979) The determination of naproxen by spectrofluorometry and its binding to serum proteins. *Acta Pharmacol Toxicol (Copenh)* **44:**277-283.

Renton KW (2005) Regulation of drug metabolism and disposition during inflammation and infection. *Expert Opin Drug Metab Toxicol* **1:**629-640.

Ricciotti E and FitzGerald GA (2011) Prostaglandins and inflammation. *Arterioscler Thromb Vasc Biol* **31:**986-1000.

Rodgers T, Leahy D, and Rowland M (2005) Physiologically based pharmacokinetic modeling 1: predicting the tissue distribution of moderate-to-strong bases. *J Pharm Sci* **94:**1259-1276.

Rodgers T and Rowland M (2006) Physiologically based pharmacokinetic modelling 2: predicting the tissue distribution of acids, very weak bases, neutrals and zwitterions. *J Pharm Sci* **95:**1238-1257.

Runkel R, Forchielli E, Sevelius H, Chaplin M, and Segre E (1974) Nonlinear plasma level response to high doses of naproxen. *Clin Pharmacol Ther* **15:**261-266.

Segre EJ (1975) Naproxen metabolism in man. *J Clin Pharmacol* **15:**316-323.

Shah DK and Betts AM (2012) Towards a platform PBPK model to characterize the plasma and tissue disposition of monoclonal antibodies in preclinical species and human. *J Pharmacokinet Pharmacodyn* **39:**67-86.

Shi X, Shang W, Wang S, Xue N, Hao Y, Wang Y, Sun M, Du Y, Cao D, Zhang K, and Shi Q (2015) Simultaneous quantification of naproxcinod and its active metabolite naproxen in rat plasma using LC-MS/MS: application to a pharmacokinetic study. *J Chromatogr B Analyt Technol Biomed Life Sci* **978-979:**157-162.

Simkin PA (1979) Synovial permeability in rheumatoid arthritis. *Arthritis Rheum* **22:**689-696.

Slaviero KA, Clarke SJ, and Rivory LP (2003) Inflammatory response: an unrecognised source of variability in the pharmacokinetics and pharmacodynamics of cancer chemotherapy. *Lancet Oncol* **4:**224-232.

Smith WL, DeWitt DL, and Garavito RM (2000) Cyclooxygenases: structural, cellular, and molecular biology. *Annu Rev Biochem* **69:**145-182.

Stoeckel K, McNamara PJ, Brandt R, Plozza-Nottebrock H, and Ziegler WH (1981) Effects of concentration-dependent plasma protein binding on ceftriaxone kinetics. *Clin Pharmacol Ther* **29:**650-657.

Stuart JM, Cremer MA, Townes AS, and Kang AH (1982) Type II collagen-induced arthritis in rats. Passive transfer with serum and evidence that IgG anticollagen antibodies can cause arthritis. *J Exp Med* **155:**1-16.

van den Ouweland FA, Franssen MJ, van de Putte LB, Tan Y, van Ginneken CA, and Gribnau FW (1987) Naproxen pharmacokinetics in patients with rheumatoid arthritis during active polyarticular inflammation. *Br J Clin Pharmacol* **23:**189-193.

van Vollenhoven RF (2009) Sex differences in rheumatoid arthritis: more than meets the eye. *BMC Med* **7:**12.

Vane JR (1971) Inhibition of prostaglandin synthesis as a mechanism of action for aspirin-like drugs. *Nat New Biol* **231:**232-235.

Vree TB, van den Biggelaar-Martea M, Verwey-van Wissen CP, Vree JB, and Guelen PJ (1993) Pharmacokinetics of naproxen, its metabolite O-desmethylnaproxen, and their acyl glucuronides in humans. *Biopharm Drug Dispos* **14:**491-502.

Wallis WJ, Simkin PA, and Nelp WB (1985) Low synovial clearance of iodide provides evidence of hypoperfusion in chronic rheumatoid synovitis. *Arthritis Rheum* **28:**1096-1104.

Watson DJ, Rhodes T, Cai B, and Guess HA (2002) Lower risk of thromboembolic cardiovascular events with naproxen among patients with rheumatoid arthritis. *Arch Intern Med* **162:**1105-1110.

Wilkinson P, Jeremy R, Brooks FP, and Hollander JL (1965) The Mechanism of Hypoalbuminemia in Rheumatoid Arthritis. *Ann Intern Med* **63:**109-114.

Wong BK, Bruhin PJ, and Lin JH (1999) Dose-dependent plasma clearance of MK-826, a carbapenem antibiotic, arising from concentration-dependent plasma protein binding in rats and monkeys. *J Pharm Sci* **88:**277-280.

Footnotes

We thank the China Scholarship Council for providing the financial support for Xiaonan Li to pursue research at the State University of New York at Buffalo. We thank Donna Ruszaj for technical assistance with LC-MS/MS assay development**.** This work was funded by the National Institute of General Medical Sciences [Grant GM24211].

Figure Legends

Figure 1. The pharmacokinetic model for naproxen incorporating protein binding in the central and peripheral compartments. Symbols are defined in the text and Tables 1 and 5.

Figure 2. Plasma albumin concentrations in CIA males (CM), healthy males (HM), CIA females (CF) and healthy females (HF) determined by ELISA. a and b: *** $P < 0.001$, significant difference compared with CM and HF; c: *** $P < 0.001$, significant difference compared with HF; d: ** $P < 0.01$, significant difference compared with CM.

Figure 3. Rosenthal plots of bound/unbound concentrations (C_b/C_f) versus unbound concentrations (C_f) for NPX binding in rat plasma. Embedded figures are plots of free fractions (f_u) versus total concentrations (C_t) for NPX binding. Closed circles depict CIA rats, open circles depict healthy rats.

Figure 4. Relationship of bound (C_b) versus unbound (C_f) concentrations of NPX in the four groups. Curves depict fitting of data using Eq. 1.

Figure 5. Plasma concentration versus time profiles of 10 mg/kg (solid circles and solid lines), 25 mg/kg (open squares and long dashed lines) and 50 mg/kg (solid triangles and short dashed lines) NPX in female (left panel) and male (right panel) arthritic rats. Symbols are observed total plasma concentrations of NPX. Curves in the upper panel depict model fittings jointly for all dose groups. Curves in the lower panel depict model-predicted unbound plasma concentrations of NPX.

Figure 6. Plasma concentration versus time profiles of 50 mg/kg NPX in female and male healthy rats. Symbols are observed total plasma concentrations of NPX. Dashed lines depict model fittings jointly for all groups, and solid lines depict model-predicted unbound plasma concentrations of NPX.

Figure 7. Simulated unbound plasma NPX concentration versus time profiles for 50 mg/kg dose groups. Solid lines depict profiles for arthritic rats and dashed lines reflect healthy rats.

Table 1

Parameter estimations for plasma protein binding of NPX

Parameters	Definition	Estimates (CV%)			
		CIA females	Healthy females	CIA males	Healthy males
Ka_1 (μM^{-1})	Association constant for first binding site	0.28 (3.53)	0.25 (3.33)	0.26 (4.00)	0.26 (1.50)
Ka_2 (μM^{-1})	Association constant for second binding site	0.0041 (4.2)	0.0043 (4.35)	0.0056 (11.75)	0.0054 (2.65)
n_1	Number of first class binding sites	1 (Fixed)			
n_2	Number of second class binding sites	4 (Fixed)			
Pt (μM)	Measured albumin concentration	347 (Fixed)	550 (Fixed)	282 (Fixed)	422 (Fixed)
n_1Pt [a] (μM)	Binding capacity of first binding site	347	550	282	422
n_2Pt [a] (μM)	Binding capacity of second binding site	1388	2200	1128	1688

[a] Binding capacities were calculated as the product of $n_i \times Pt$.

Table 2

NCA pharmacokinetic parameters based on total NPX concentrations for 10, 25 and 50 mg/kg IP doses in CIA rats (Mean ± SD)

Dose (mg/kg)	CIA Females (n=3)				CIA Males (n=3)			
	Dose-normalized AUC (μg·h·kg/mL/mg)	*CL/F* (mL/h/kg)	*V/F* (mL/kg)	$t_{1/2}$ (h)	Dose-normalized AUC (μg·h·kg/mL/mg)	*CL/F* (mL/h/kg)	*V/F* (mL/kg)	$t_{1/2}$ (h)
10	33.84 ± 5.17	29.98 ± 4.21	133.8 ± 23.61	3.13 ± 0.65	27.09 ± 1.39	36.98 ± 1.85	135.1 ± 16.32	2.54 ± 0.31
25	25.44 ± 0.8	39.34 ± 1.22*	157.0 ± 15.13	2.76 ± 0.23	24.26 ± 1.35	41.31 ± 2.38	137.9 ± 10.73	2.32 ± 0.18
50	18.74 ± 0.86**	53.43 ± 2.53**	287.1 ± 42.50**	3.74 ± 0.64	16.20 ± 1.22**	61.99 ± 4.87**	229.3 ± 48.93*	2.55 ± 0.36

*P<0.05, **P<0.01, significant difference compared with 10 mg/kg dose group in each sex group.

DMD Fast Forward. Published on February 28, 2017 as DOI: 10.1124/dmd.116.074500
This article has not been copyedited and formatted. The final version may differ from this version.

Table 3

Comparison of NCA pharmacokinetic parameters based on total NPX concentrations for 50 mg/kg IP doses in CIA and healthy rats (Values are Mean ± SD)

Groups	n	AUC (μg·h/mL)	*CL/F* (mL/h/kg)	*V/F* (mL/kg)	$t_{1/2}$ (h)
CIA males	3	809.8 ± 61.0*	61.99 ± 4.87**	229.3 ± 48.9*	2.55 ± 0.36
Healthy males	4	1054.5 ± 116.5	47.76 ± 4.98	169.7 ± 18.2	2.46 ± 0.03
CIA females	3	936.0 ± 42.2*	53.43 ± 2.53*	287.1 ± 42.5*	3.74 ± 0.64
Healthy females	4	1203.4 ± 138.2	41.89 ± 4.51	188.6 ± 24.7	3.13 ± 0.34

* $P < 0.05$, ** $P < 0.01$, significant difference compared with healthy group in each sex group.

DMD Fast Forward. Published on February 28, 2017 as DOI: 10.1124/dmd.116.074500
This article has not been copyedited and formatted. The final version may differ from this version.

Table 4

Modeled pharmacokinetic parameter estimates for unbound NPX after IP administration

Parameters	Definition	Estimates	CV %
k_a (1/h)	Absorption rate constant	0.814	7.54
$CL_{Arthritic}$ (mL/h/kg)	Unbound plasma clearance in arthritic rats	1370	4.73
$CL_{Healthy}$ (mL/h/kg)	Unbound plasma clearance in healthy rats	1879	9.26
V_p (mL/kg)	Central volume of distribution	32.36 [a]	Fixed
$CL_{d\ Arthritic}$ (mL/h/kg)	Unbound distribution clearance in arthritic rats	647.2	18.61
$CL_{d\ Healthy}$ (mL/h/kg)	Unbound distribution clearance in healthy rats	1371	45.23
$V_{t\ Arthritic}$ (mL/kg)	Peripheral distribution volume in arthritic rats	140.7	9.27
$V_{t\ Healthy}$ (mL/kg)	Peripheral distribution volume in healthy rats	114.7	17.37

[a] Physiological parameter values obtained from (Shah and Betts, 2012).

DMD Fast Forward. Published on February 28, 2017 as DOI: 10.1124/dmd.116.074500
This article has not been copyedited and formatted. The final version may differ from this version.

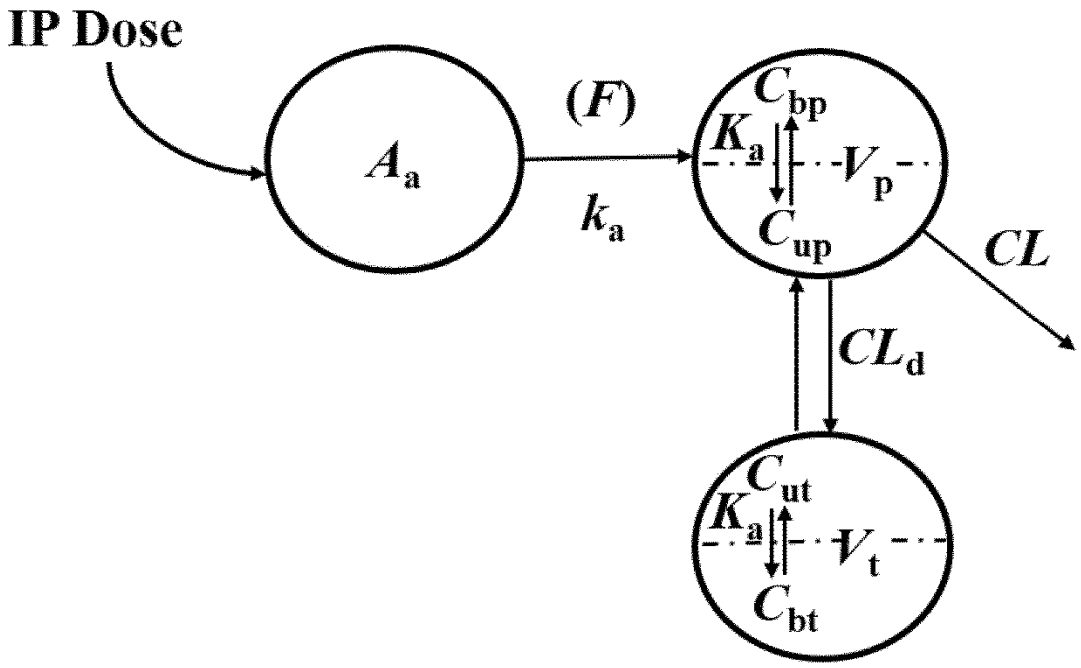

Figure 1

DMD Fast Forward. Published on February 28, 2017 as DOI: 10.1124/dmd.116.074500
This article has not been copyedited and formatted. The final version may differ from this version.

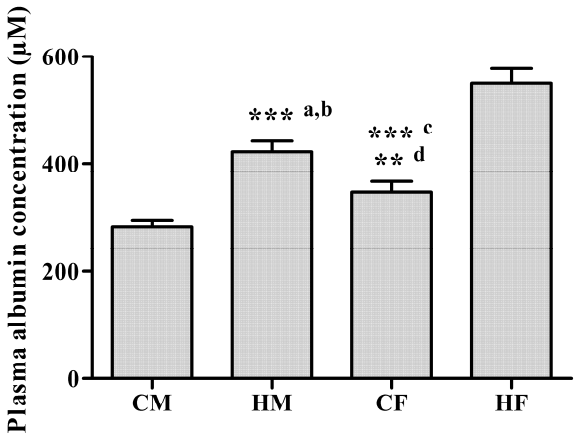

Figure 2

DMD Fast Forward. Published on February 28, 2017 as DOI: 10.1124/dmd.116.074500
This article has not been copyedited and formatted. The final version may differ from this version.

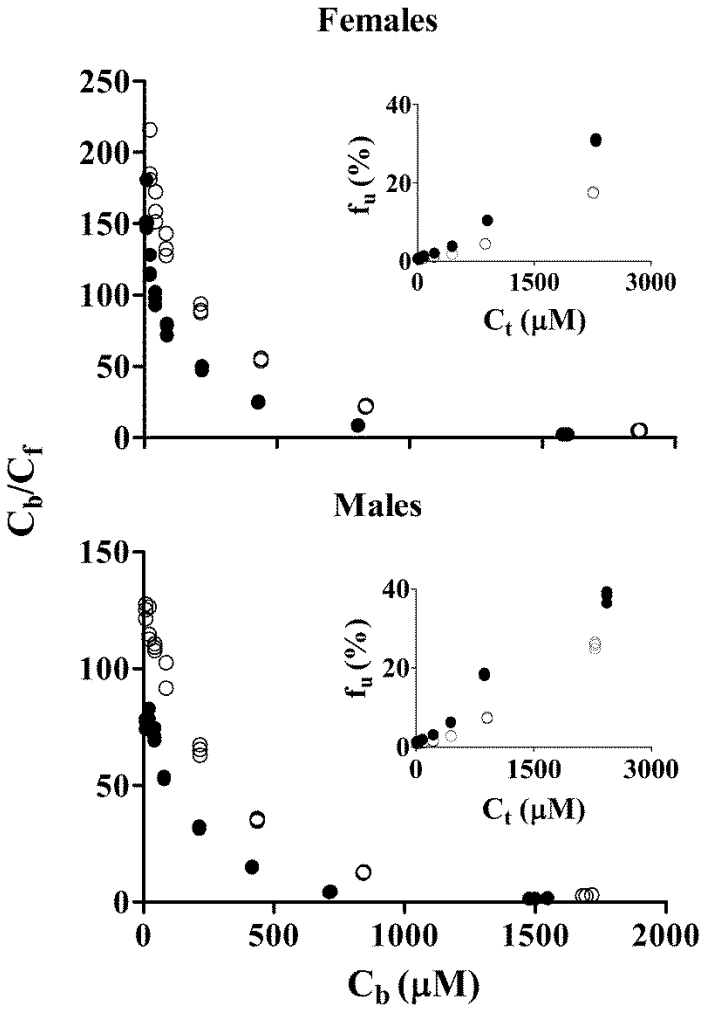

Figure 3

DMD Fast Forward. Published on February 28, 2017 as DOI: 10.1124/dmd.116.074500
This article has not been copyedited and formatted. The final version may differ from this version.

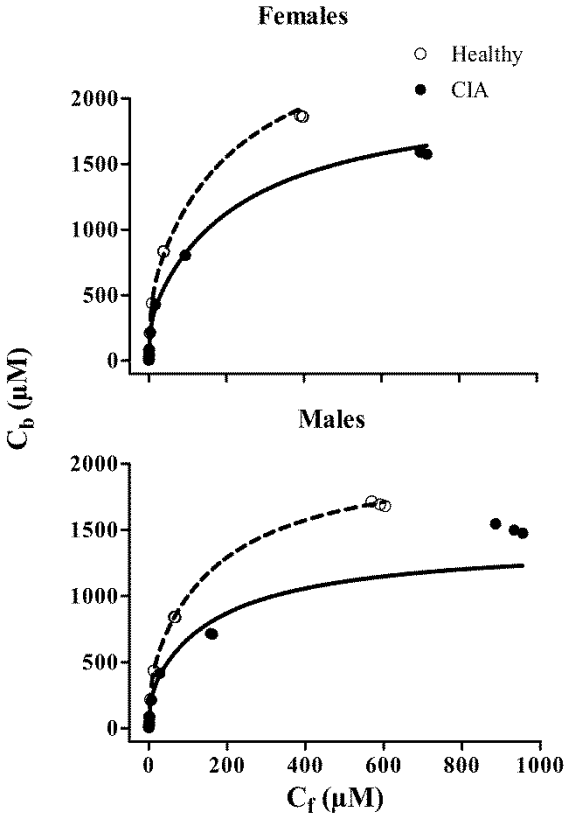

Figure 4

DMD Fast Forward. Published on February 28, 2017 as DOI: 10.1124/dmd.116.074500
This article has not been copyedited and formatted. The final version may differ from this version.

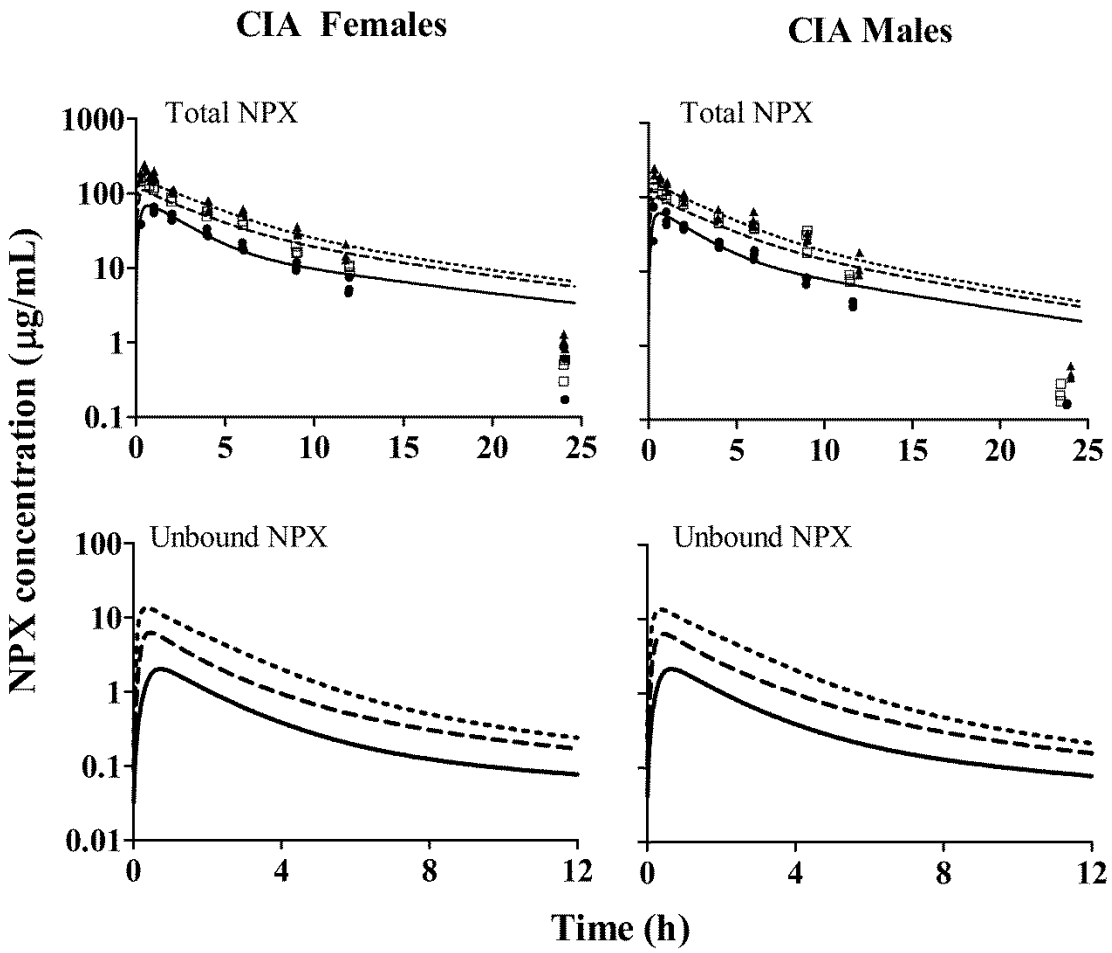

Figure 5

DMD Fast Forward. Published on February 28, 2017 as DOI: 10.1124/dmd.116.074500
This article has not been copyedited and formatted. The final version may differ from this version.

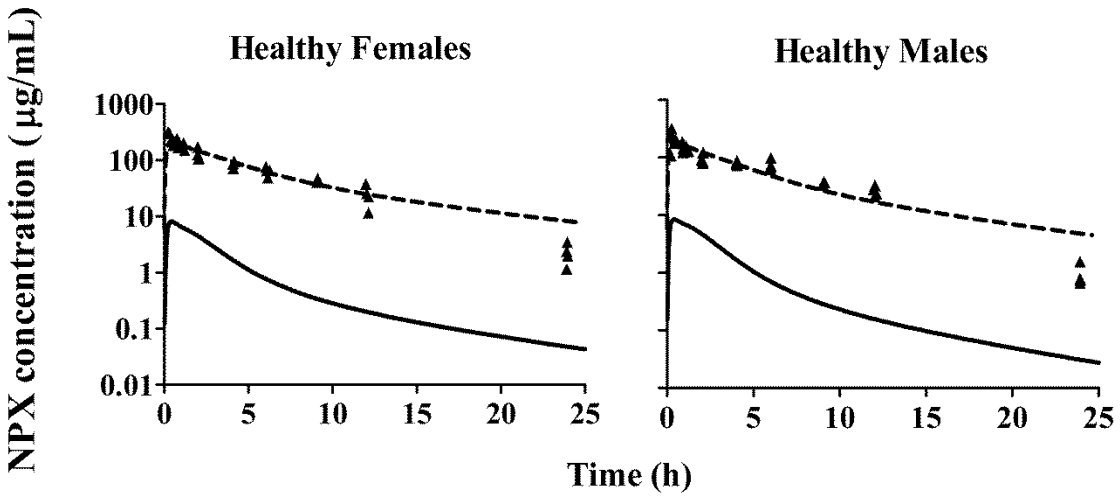

Figure 6

DMD Fast Forward. Published on February 28, 2017 as DOI: 10.1124/dmd.116.074500
This article has not been copyedited and formatted. The final version may differ from this version.

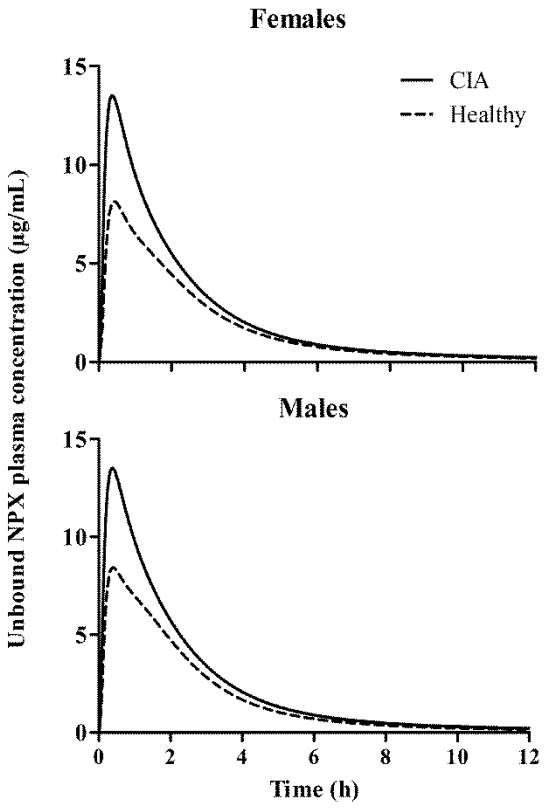

Figure 7